The Journal of Microbiology (2012) Vol. 50, No. 3, pp. 502–510
DOI 10.1007/s12275-012-2090-9

Effect of *Salmonella* Treatment on an Implanted Tumor (CT26) in a Mouse Model

Misun Yun[1], SangO Pan[2], Sheng- Nan Jiang[3], Vu Hong Nguyen[3], Seung-Hwan Park[3], Che-Hun Jung[5], Hyung-Seok Kim[4], Jung-Joon Min[3], Hyon E. Choy[1], and Yeongjin Hong[1]*

[1]Departments of Microbiology, Chonnam National University Medical School, Gwangju 501-746, Republic of Korea
[2]Jeollanamdo Institute of Natural Resources Research (JINR), Jeollanamdo 529-851, Republic of Korea
[3]Departments of Nuclear Medicine, [4]Forensic Medicine, Chonnam National University Medical School, Gwangju 501-746, Republic of Korea
[5]Departments of Chemistry, Chonnam National University, Gwangju 500-757, Republic of Korea

(Received February 16, 2012 / Accepted March 14, 2012)

The use of bacteria has contributed to recent advances in targeted cancer therapy especially for its tumor-specific accumulation and proliferation. In this study, we investigated the molecular events following bacterial therapy using an attenuated *Salmonella* Typhimurium defective in ppGpp synthesis (ΔppGpp), by analyzing those proteins differentially expressed in tumor tissues from treated and untreated mice. CT26 murine colon cancer cells were implanted in BALB/c mice and allowed to form tumors. The tumor-bearing mice were treated with the attenuated *Salmonella* Typhimurium. Tumor tissues were analyzed by 2D-PAGE. Fourteen differentially expressed proteins were identified by mass spectrometry. The analysis revealed that cytoskeletal components, including vimentin, drebrin-like protein, and tropomyosin-alpha 3, were decreased while serum proteins related to heme or iron metabolism, including transferrin, hemopexin, and haptoglobin were increased. Subsequent studies revealed that the decrease in cytoskeletal components occurred at the transcriptional level and that the increase in heme and iron metabolism proteins occurred in liver. Most interestingly, the same pattern of increased expression of transferrin, hemopexin, and haptoglobin was observed following radiotherapy at the dosage of 14 Gy.

Keywords: *Salmonella* Typhimurium, bacterial tumor targeting, CT26, protein response

*For correspondence. E-mail: yjhong@chonnam.ac.kr; Tel.: +82-61-379-8478; Fax: +82-61-379-8455

Introduction

Several bacterial strains, including *Salmonella*, *Clostridium*, *Bifidobacterium*, *Listeria*, *Vibrio*, and *E. coli*, selectively target and proliferate in solid tumors in mouse models (Kimura *et al.*, 1980; Pawelek *et al.*, 1997; Agrawal *et al.*, 2004; Yu *et al.*, 2004; Zhao *et al.*, 2005; Taniguchi *et al.*, 2010). Bacterial cancer therapy has been developed by taking advantage of these bacterial properties. Recently, this therapy has been clinically tested in canine and even human patients (Toso *et al.*, 2002; Thamm *et al.*, 2005). In addition, bacterial therapy has revealed additive antitumor efficacy in combination with other cancer therapies, including radio-, chemo-, and immunotherapy, which further demonstrated its practical use for tumor therapy in the near future (Jain and Forbes, 2001; Ryan *et al.*, 2006; Jiang *et al.*, 2010). As cancer therapeutic agents, bacteria possess several advantages including that it can be engineered to express genes encoding imaging probes and/or therapeutic proteins (Weibel *et al.*, 2008; Ryan *et al.*, 2009; Jiang *et al.*, 2010; Min *et al.*, 2010; Nguyen *et al.*, 2010).

Intravenously injected bacteria accumulate initially in liver and spleen but vanish in two or three days, presumably due to host immune function (Min *et al.*, 2008a, 2008b; Weibel *et al.*, 2008). Those bacteria that accumulate in a tumor mass, however, not only survive but also proliferate therein, which could result in tumor regression depending on the bacterial strain. Facultative anaerobes such as *E. coli* and *Salmonella* spp. have been shown to proliferate selectively in hypoxic and necrotic regions in the tumor (Pawelek *et al.*, 1997; Low *et al.*, 2004; Yu *et al.*, 2004; Zhao *et al.*, 2005). Interestingly, bacterial therapy with *Salmonella* Typhimurium but not with *E. coli*, results in tumor regression (Jiang *et al.*, 2010).

Despite the continuing interest in bacterial cancer therapy, little is known about the molecular events at the transcription or translation level in the tumor tissue having undergone bacterial therapy. In an attempt to investigate the molecular events relative to the mechanisms of tumor regression, differentially expressed host proteins were identified in tumors targeted by Typhimurium. We have previously reported that *S. typhimurium* defective in the biosynthesis of ppGpp (ΔppGpp strain), a global regulator of virtually all virulence genes, is highly attenuated (Song *et al.*, 2004; Na *et al.*, 2006), but is capable of targeting CT26 colon tumors in mice, leading to a retardation of tumor growth (Nguyen *et al.*, 2010). In the present study, proteins differentially expressed in CT26 tumors after the *Salmonella* (ΔppGpp strain) treatment were identified by proteomic analysis.

Materials and Methods

Bacterial strains and cell lines

The attenuated *S. typhimurium* strains SHJ2037 and A1R were cultured in Luria-Bertani (LB) broth medium (Difco Laboratories, USA) with vigorous aeration at 37°C, as previously described (Na *et al*., 2006; Zhao *et al*., 2006). SHJ2037 (*relA*::*cat*, *spoT*::*kan*) is a ΔppGpp strain and A1R is an auxotrophic mutant for leucine and arginine, kindly provided by R. M. Hoffman (AntiCancer, Inc., USA) (Zhao *et al*., 2006). To non-invasively monitor the bacterial targeting of tumor tissue in mice, the bacterial luciferase (lux) operon from *S. typhimurium*-Xen26 (Caliper) was transduced into the ΔppGpp strain by P22HT *int* transduction (ΔppGpp-Lux) (Nguyen *et al*., 2010). The mouse cell lines, CT26 (colon carcinoma), 4T1 (breast cancer), and B16F10 (melanoma), were grown in high-glucose Dulbecco's modified Eagle medium (DMEM) containing 10% FBS and 1% penicillin-streptomycin.

Generation of tumor-bearing mice

Five to six week-old male BALB/c mice (20–30 g body weight) were purchased from the Orient Company (Seoul, Korea). The mice carrying subcutaneous tumors were generated as described (Min *et al*., 2008a). In brief, CT26 cells were harvested and 1×10^6 cells were suspended in 50 μl PBS and injected subcutaneously into the right thigh of each mouse.

Optical bioluminescence imaging

To obtain images of bacterial bioluminescence, anesthetized animals were placed in the light-tight chamber of the IVIS100 imaging system (Caliper, USA), equipped with a cooled charge-coupled device (CCD) camera (Min *et al*., 2008b). Photons emitted from luciferase-expressing bacteria were collected and integrated over one-minute periods.

Protein extraction

At sacrifice, tumor tissues were isolated, weighed, mixed in three volumes of protein extraction buffer (8 M urea, 2 M thiourea) and homogenized. After centrifugation (8,000 rpm, 30 min), the supernatant was collected and mixed with the same volume of 20% TCA/acetone to precipitate the proteins (-20°C, 1 h). The TCA was washed away with cold acetone (3 times) and the proteins were collected by centrifugation (10,000 rpm, 15 min, 4°C). The precipitate was dried, dissolved in 200 μl protein extraction buffer and stored at -70°C. Protein quantification was conducted using the BCA method (Bensadoun and Weinstein, 1976) with bovine serum albumin and confirmed with Western blotting against actin.

Two-dimensional gel electrophoresis (2-DE)

The proteins were separated in 2D-PAGE and analyzed by MADLI-TOF mass spectrometry as described (Granvogl *et al*., 2007). The extracted proteins were solubilized with 200 μl of rehydration buffer containing 8 M urea, 2% CHAPS, 2% IPG buffer, 100 mM DTT, and 0.001% bromophenol blue. 250 μl of rehydration buffer containing 1 mg of protein was applied on immobilized pH 4–7 (NL) gradient (IPG) dry strip (13 cm) (GE Healthcare, UK) and then the IPG strip was rehydrated for 12 h at 20°C. After rehydration, proteins were focused by IEF (isoelectric focusing). The voltage was 300 V for 1 h, 3500 V for 90 min, and 3500 V for 4 h. The current was limited to 2 mA per strip. Following IEF, the resulting strip was equilibrated for reduction of proteins with equilibration buffer (50 mM Tris-Cl; pH 8.8, 6 M urea, 30% glycerol, 2% SDS, 0.001% bromophenol blue, and 1% DTT) for 20 min at room temperature and then incubated for proteins to be alkylated with equilibration buffer containing 2.5% IAA (iodoacetamide) but not DTT, in the dark, for 20 min at room temperature. The strips were separated on a 12% gel by the second-dimension of electrophoresis and run in 45 mA at 20°C. To ensure reproducibility in the gel pattern, we repeated the 2-dimentional gel electrophoresis against the same sample 3 times.

Gel Staining and Detection of Proteins: The resulting gel was fixed in 12% trichloacetic acid for 1 h, and stained with Coomassie Blue G250 according to the colloidal Coomassie staining method. To identify the spots of interest, gels were excised and transferred into a microcentrifuge tube and then rinsed with distilled water for 15 min. 50% acetonitrile (ACN) was added to the tube and incubated for 15 min. On discarding the ACN, 100% ACN was added to the tube and allowed to stand for 15 min until gel pieces became white and had shrunk. After removal of ACN, the gel was incubated with 100 mM ammonium bicarbonate (ambic) for 5 min. 100% ACN was added to the tube and incubated for 15 min. This procedure was repeated until dye was no longer visible. Destained gel pieces were dried using a Speed Vac. Dried gel pieces can be stored at -70°C prior to use.

Trypsin Digestion and Mass Spectrometry: Destained gel pieces were treated with 0.1% (w/v) RapiGest SF in 50 mM ambic buffer for 10 min at 37°C and then dried using a Speed Vac. Gel pieces were treated with 30 μl of trypsin solution (10 μg/ml) and incubated for 45 min on ice. After discarding excess trypsin solution, 30 μl of hydrolysis buffer (50 mM ambic / 1 mM $CaCl_2$) was added to the tube containing the gel piece. Finally, the gel pieces were incubated overnight at 37°C. Tryptic peptides were transferred into a new microcentrifuge tube and 20 μl of 50 mM ambic buffer was added to the tube containing the gel piece for 15 min. 20 μl of ACN was added to the tube containing the gel piece, incubated for 15 min, and then 40 μl of the eluted peptides were collected into the new tube containing tryptic peptides. Gel pieces were also incubated with 20 μl of 5% formic acid for 15 min and with 20 μl of ACN was added to the gel tube. The 5% formic acid/ACN (ratio 1:1) step was repeated to elute tryptic peptides. After adding 100 mM DTT to the tryptic peptides to a final concentration of 1 mM, the peptides was dried by using a vacuum centrifuge and stored at -70°C for further analysis. The dried peptides were dissolved with 3 μl of buffer (50% ACN/ 0.1% TFA). 1 μl of peptide solution was mixed with 1 μl of CHCA matrix solution (10 mg/ml of CHCA, 50% ACN, 49.9% EtOH, and 0.1% TFA), then 1 μl of the sample/matrix mixture was directly deposited onto the plate and dried. Protein identification by peptide mass fingerprinting (PMF) was carried out using

Table 1. Primer sets used in real-time RT-PCR analysis

Gene	Primer sequences
VIME	Forward: 5′-TGCTGCCCTGCGTGATGTGC
	Reverse: 5′-TGGCGCTCCAGGGACTCGTT
DBNL	Forward: 5′-TCCAGGATGTAGGGCCGCAGG
	Reverse: 5′-TCCTGCTGGAAGGGCTCGGG
TPM3	Forward: 5′-GCTGGCAGAGTCCCGTTGCC
	Reverse: 5′-TCAGGTCCAGCAGGGTCTGGT
HPT	Forward: 5′-GCT GCC CAA ACG CCC CAG AG
	Reverse: 5′-GGT GAG TCC GTG GCG GGA GA
HEMO	Forward: 5′-CGC GGT GCC ACC TAT GCC TT
	Reverse: 5′-AGG TGA TCC CAG GAG GGC T
TF	Forward: 5′-GCT GCG CTC CCG GGT ATG AG
	Reverse: 5′-GAG CTT GGG CCA GGT GGC AG
Actin	Forward: 5′-TCA TGA AGT GTG ACG TTG ACA TCC GT
	Reverse: 5′-CTT AGA AGC ATT TGC GGT GCA CGA TG

the MASCOT database (matrixscience.com). The parameters for PMF were as follows: mass error tolerance: 100 ppm; variable modification: oxidation of methionine, and carbamidomethylation of cysteine; the number of missed cleavages: 1. The mass data were calibrated with Angiotensin I (*m/z* 1296.6853) as an external standard and a peptide derived from trypsin (*m/z* of 2211.1046) as internal standard.

Western blot analysis

Total proteins (100 μg) were separated by electrophoresis on 10% SDS-polyacrylamide gel. Proteins were transferred to nitrocellulose membranes (Bio-Rad, USA) and the membranes were probed with antibodies against vimentin (1:500, BD Biosciences, USA), drebrin-like (1:500, Proteintech Group, USA), tropomyosin alpha 3 (1:1000, Santa Cruz Biotechnology, USA), transferrin (1:1000, Novos Biologicals, USA), hemopexin (1:500, Life Diagnostics, USA), haptoglobin (1:500, Life Diagnostics) and actin (1:1000, Sigma, USA). Species-appropriate secondary antibodies were used for visualization. After adding luminol reagent (Santa Cruz Biotechnology), immunoreactive proteins were imaged and quantified with a LAS-3000 Imager (Fujifilm, Japan).

Real-time reverse transcriptase polymerase chain reaction (RT-PCR) analysis

Total RNA was extracted from frozen tumor tissues using the Trizol method (QIAGEN, USA). The concentration of RNA was quantified by spectrometry. Single-stranded cDNAs were synthesized from 500 ng of total RNA using a 1st strand cDNA synthesis kit (TaKaRa, Japan). Relative transcript abundance was measured with the LightCycler (Roche, Switzerland) against cDNAs, using the SYBR premix Ex-Taq (TaKaRa). Primer sequences are shown in Table 1.

Radiation therapy

Radiotherapy was done as described (Jiang *et al.*, 2010). Tumors were irradiated twice, with a 4-day interval (2×7 Gy).

Statistical analyses

Following two-dimensional gel electrophoresis, quantitative analysis of protein spots on the gels was performed using the Phoretix 2D software (Nonlinear Dynamics, USA).

Results

Tumor tissue targeted by ΔppGpp-Lux *S. typhimurium*

We injected the bioluminescent *S. typhimurium* (ΔppGpp-Lux, 4×10^7 CFU) into the tail vein of BALB/c mice implanted with CT26 tumors, when the tumors reached a size of ~150 mm^3 (Nguyen *et al.*, 2010). Three days after injection, the CT26 tumor volume decreased to 37% of its initial volume (Fig. 1A), which is consistent with previous results (Nguyen *et al.*, 2010). To assess bacterial localization, bioluminescence was detected in mice using a cooled CCD camera (Fig. 1B). A strong light signal was detected only in the tumor tissue, while no signal was detected in the untreated control mice. Thus, the *Salmonella* injected via the tail vein successfully targeted and proliferated in the tumor tissue, resulting in a reduction of tumor size.

Proteomic and genomic analysis of CT26 tumor tissue after ΔppGpp-Lux *S. typhimurium* injection

In an attempt to identify proteins associated with tumor regression following *Salmonella* colonization, the protein expression profile of the tumor cells was analyzed by 2D gel. Proteins were purified from tumor tissues isolated from untreated control mice and from mice that had undergone bacterial therapy. The proteins were resolved by 2D-PAGE (Fig. 2). The protein profile revealed that several proteins had decreased while others had increased in treated tumors compared to untreated tumors (Fig. 2A). Indicated by Arabic numbers are the protein spots that show changes in intensity over 2-fold. These were selected for further analysis. Of 14 protein spots selected, 8 spots showed decreased in-

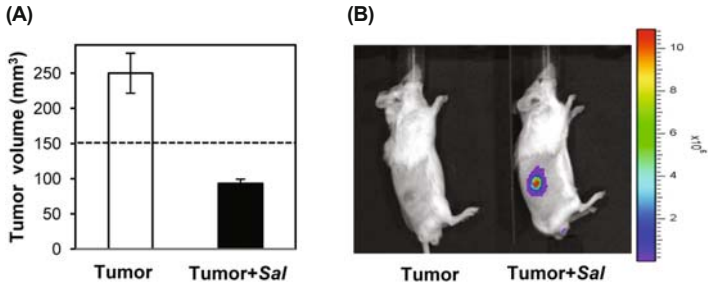

Fig. 1. Proteomic analysis of CT26 tumor tissue treated with ΔppGpp-Lux *S. typhimurium*. BALB/c mice (n=5 per group) carrying implanted CT26 cells (1×10^6) were treated with light-emitting ΔppGpp-Lux *S. typhimurium* (4×10^7 CFU). Control mice with a CT26 tumor were injected with PBS. (A) Tumor volume at day 3 post bacterial injection. Tumor, tumor from untreated control mouse; Tumor+*Sal*, tumor from mouse having undergone bacterial therapy. (B) Bioluminescent imaging of CT26 tumor-bearing mice at day 3 post bacterial treatment.

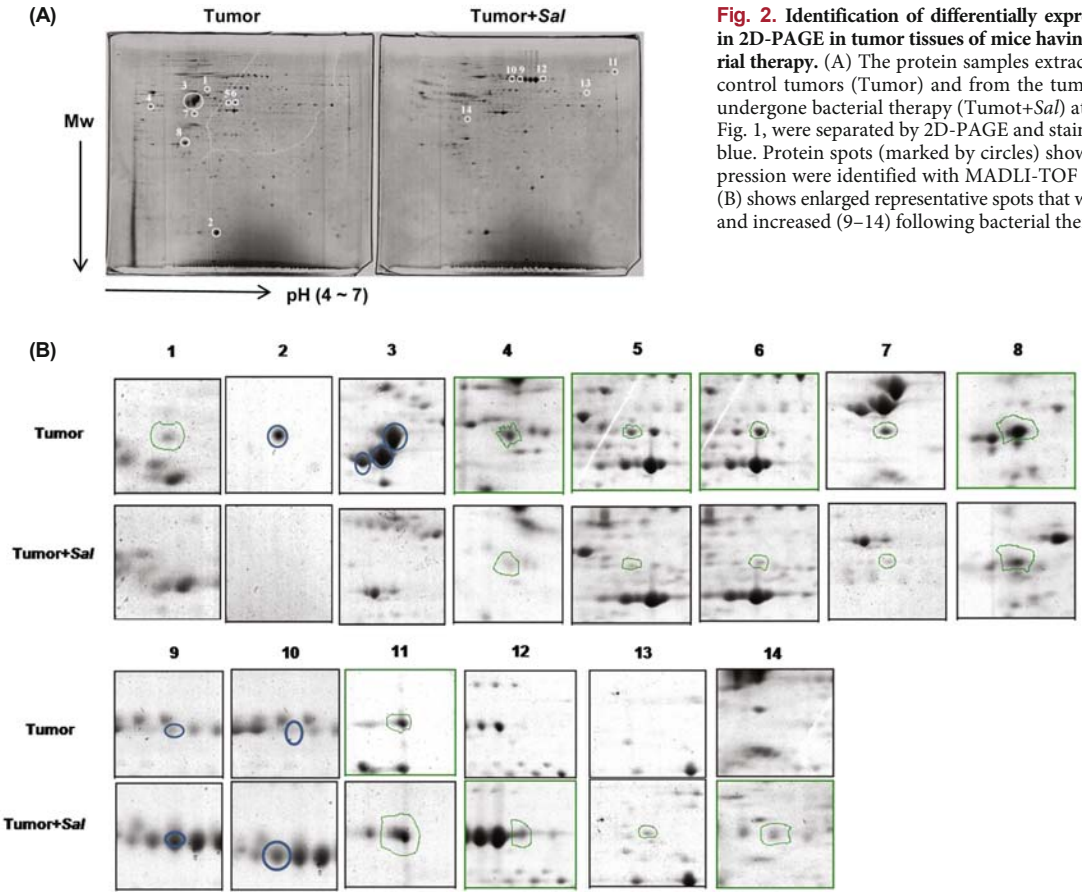

Fig. 2. Identification of differentially expressed protein spots in 2D-PAGE in tumor tissues of mice having undergone bacterial therapy. (A) The protein samples extracted from untreated control tumors (Tumor) and from the tumors of mice having undergone bacterial therapy (Tumot+*Sal*) at day 3, as shown in Fig. 1, were separated by 2D-PAGE and stained with Coomassie blue. Protein spots (marked by circles) showing differential expression were identified with MADLI-TOF mass spectrometry. (B) shows enlarged representative spots that were decreased (1–8) and increased (9–14) following bacterial therapy, respectively.

tensity and 6 spots showed increased intensity in treated tumors (Fig. 2B). The 14 proteins were identified by MALDI-TOF mass spectrometry and peptide mass fingerprinting (Table 2). Three of the proteins showing decreased expression were associated with the cytoskeleton including vimentin (VIME), drebrin-like (DBNL), and tropomyosin alpha-3 (TPM3) (Clayton *et al*., 1988; Katsumoto *et al*., 1990; Fuchs and Weber, 1994; Han *et al*., 2005). This was confirmed and quantified by Western blot analysis using specific antibodies (Fig. 3A). The protein level of VIME, DBNL, and TPM3 decreased by 3.5-, 9.28-, and 2-fold, respectively (Fig. 3B). The mRNA expression was subsequently meas-

Table 2. Differentially expressed proteins in CT26 tumor tissues at day 3 post *Salmonella* injection

no.	GenBank No.	Gene	MW/pI	Expression levels	Features
1	NP_001139780.1	DBNL	48670 / 4.90	-	Actin binding
2	NP_062615.1	STMN1	17264 / 5.76	-	Microtubule binding, oncogene
3	NP_035831.2	VIME	53655 / 5.06	-	Actin and microtubule binding, cancer marker
4	NP_031620.1	CALU	37041 / 4.49	-2.43	Calcium binding, gamma-carboxylase GGCX inhibition
5	NP_001159899.1	HNRPF	45701 / 5.31	-2.8	RNA processing
6	NP_001020013.1	HXC11	33687 / 8.68	-2.6	Transcription factor involved in development
7	NP_035159.3	RSSA	32817 / 4.80	-2.6	Ribosomal protein, receptor for bacteria
8	NP_071709.2	TPM3	32843 / 4.68	-4.6	Cytoskeleton
9	NP_033784.2	ALBU	68648 / 5.75	3	Plasma protein
10	NP_034611.2	GRP75	73483 / 5.91	3.3	Control of cell proliferation and aging
11	NP_598738.1	TF	76674 / 6.94	3.3	Iron binding, cell proliferation stimulation
12	NP_059067.2	HEMO	51308 / 7.92	2.8	Heme binding
13	NP_0320881.1	G6PD1	59225 / 6.06	+	Glucose metabolism
14	NP_0590661.1	HPT	38727 / 5.88	+	Free plasma hemoglobin binding

The protein levels in CT26 tumors at day 3 after ΔppGpp-Lux *S. typhimurium* injection were quantified relative to those in untreated control tumors. + or – with a number means increased or decreased expression, respectively, in bacteria-treated samples. + or – without any number means protein only detected in bacteria-treated samples or controls, respectively.

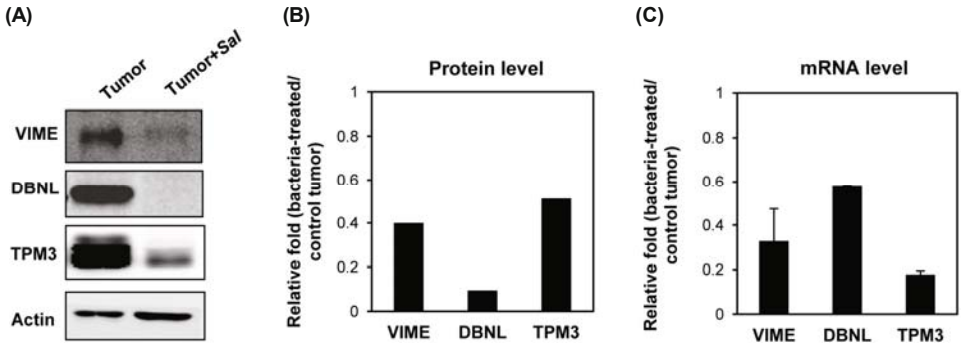

Fig. 3. Expression level of VIME, DBNL, and TPM3 in CT26 tumors treated with ΔppGpp-Lux *S. typhimurium*. The proteins extracted from tumors isolated from untreated and treated mice (day 3) were separated by 10% SDS-PAGE. Protein levels were analyzed by Western blotting using specific antibodies (A). (B) Shows quantification of band intensities in (A). The band intensity was measured with a LAS-3000 imager and normalized against actin. (C) mRNA levels following bacterial therapy. Transcript abundance was measured by real time RT-PCR (total RNA was isolated from CT26 tumors 3 days after bacterial treatment). Transcript abundance in bacteria-treated tumors is relative to control untreated tumors.

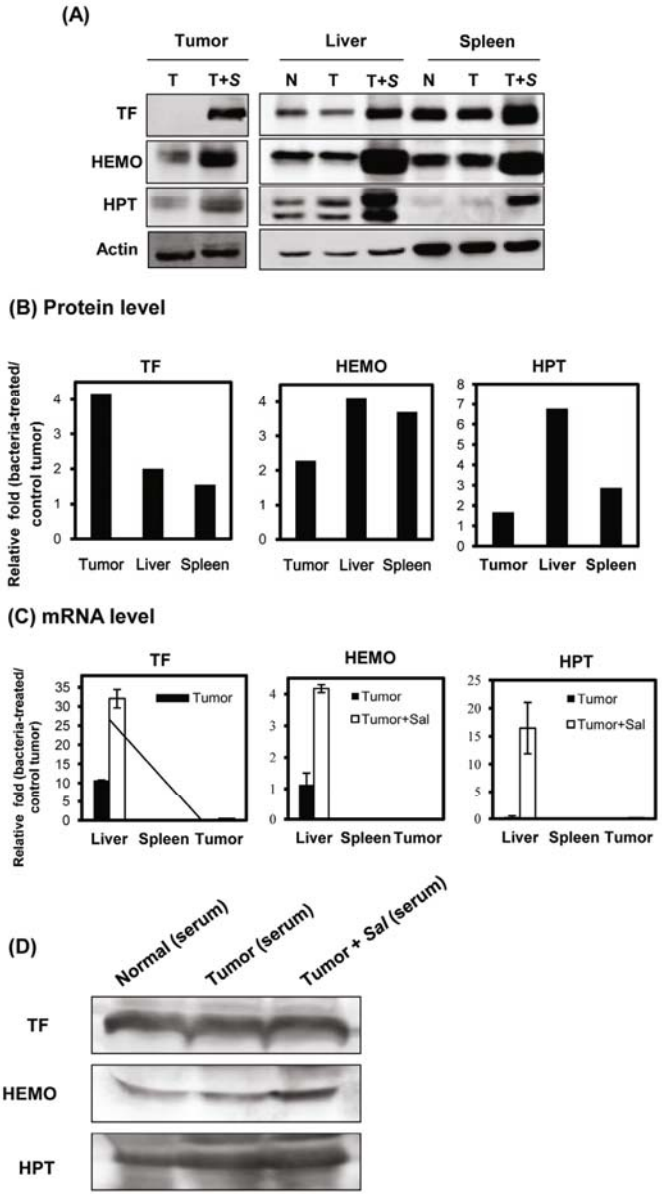

Fig. 4. Expression level of TF, HEMO, and HPT in CT26 tumor tissue, liver, spleen, and sera of mice having undergone bacterial therapy. The proteins extracted from the tissues of normal mice (N), untreated mice bearing CT26 (T) and mice bearing CT26 having undergone bacterial therapy (ΔppGpp- Lux *S. typhimurium*) (T+S) (day 3) were separated by 10% SDS-PAGE. Protein levels were analyzed by Western blotting using specific antibodies (A). (D) shows the same in the sera of treated and untreated mice. (B) shows quantification of proteins in (A): bacteria treated/untreated control. (C) mRNA levels in liver, spleen and tumor tissue following bacterial therapy. Transcript abundance was measured by real time RT-PCR (total RNA was isolated from tissues 3 days after bacterial treatment). Transcript abundance in tissues from bacteria-treated mice is relative to untreated control tumors.

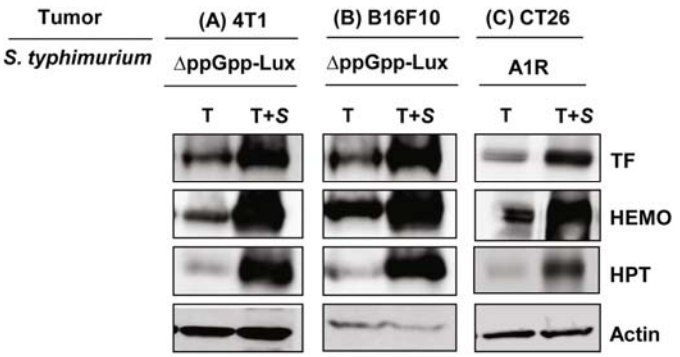

Fig. 5. Level of TF, HEMO, and HPT in various tumor tissues of mice having undergone bacterial therapy. (A) BALB/c mice (n=5 per group) were implanted with 4T1 cells (1×10^6) and treated with ΔppGpp-Lux *S. typhimurium* (4×10^7 CFU). (B) BALB/c mice (n=5 per group) were implanted with B16F10 cells (1×10^6) and treated with ΔppGpp-Lux *S. typhimurium* (4×10^7 CFU). (C) BALB/c mice (n=5 per group) were implanted with CT26 cells (1×10^6) and treated with the A1R strain of *S. typhimurium* (4×10^7 CFU). The proteins extracted from tumor tissues of untreated mice (T) and of mice having undergone bacterial therapy (T+S) (day 3) were separated by 10% SDS-PAGE. Protein levels were analyzed by Western blotting using specific antibodies.

ured by real-time RT-PCR (Fig. 3C). Results showed that protein levels correlated with transcript levels, indicating that the changes in protein expression were at the level of transcription.

Three serum proteins, transferrin (TF), hemopexin (HEMO), and haptoglobin (HPT), were increased following bacterial therapy. These proteins transport and scavenge iron and heme (Table 2) (Tolosano and Altruda, 2002; Macedo and de Sousa, 2008; Nielsen *et al*., 2010). TF, HEMO, and HPT protein levels were estimated to increase by 4.16-, 2.28-, and 1.66-fold, respectively, in treated tumors compared to untreated tumors (Figs. 4A and 4B). Because these proteins are synthesized mainly in liver and subsequently secreted into circulation (Dobryszycka, 1997; Tolosano and Altruda, 2002; Macedo and de Sousa, 2008), levels of these proteins were measured in liver and spleen by Western blot analysis. Results showed that these proteins were present at high levels in the spleens and livers of mice having undergone bacterial therapy. The mRNA expression was measured by real time RT-PCR in spleen and liver as well as in tumor (Fig. 4C). Interestingly, increased mRNA expression was only detected in the liver but not in the spleen and tumor, suggesting that these proteins were induced in liver following bacterial therapy and subsequently transported to the spleen and tumor. These proteins, belonging to class I acute-phase proteins, are produced in relation to inflammation and hypoxia. Thus, we also measured the protein levels in the animal sera by Western blot analysis (Fig. 4D). Most interestingly, we found the levels of these protein in the sera of normal mice, and untreated and treated mice were not different suggesting that the accumulation of TF, HEMO, and HPT in tumors following *Salmonella* treatment is distinctly tumor specific.

Interestingly, the same pattern of increase in TF, HEMO, and HPT in tumors following bacterial therapy was observed in different tumor types such as 4T1 (breast cancer) or B16F10 (melanoma) (Figs. 5A and 5B). Thus, increased expression of these proteins in liver and subsequent trans-

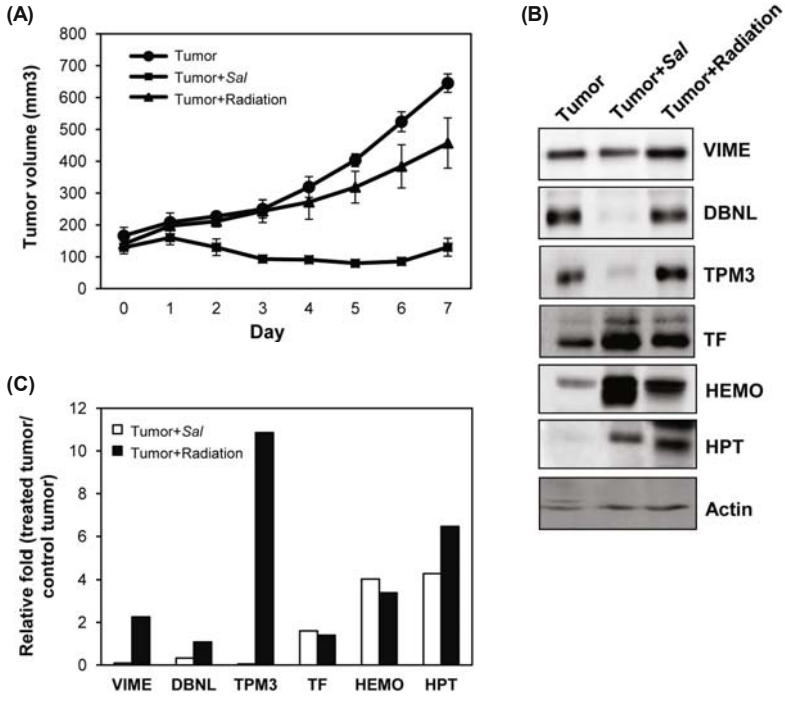

Fig. 6. Antitumor efficacy of bacterial and radiation therapy in the CT26 mouse tumor model. BALB/c mice (n=5 per group) carrying implanted CT26 cells (1×10^6) were treated with ΔppGpp-Lux *S. typhimurium* (4×10^7 CFU). For radiation therapy, tumor-bearing mice were exposed twice to 7 Gy-radiation at days 2 and 6. Control mice were injected with PBS. (A) Tumor volumes were measured daily: untreated control tumors (circles); tumors from mice having undergone radiation therapy (triangles); tumors from mice having undergone bacterial therapy (squares). (B) Protein levels from tumor tissues extracted at day 7 were analyzed by Western blotting using specific antibodies. (C) Quantification of band intensities in (B). The amounts of proteins in treated tumors were expressed relative to that in the untreated tumor.

port into tumor tissue following bacterial therapy may be a general phenomenon independent of tumor type. The same results were observed when CT26 tumors were colonized by *S. typhimurium* A1R strain, selected for enhanced targeting to prostate cancer (Song *et al.*, 2004; Zhao *et al.*, 2005), suggesting that the phenomenon is not *Salmonella* ΔppGpp strain-specific, either (Fig. 5C).

Comparison of changes in protein expression following radiotherapy and bacterial therapy

Radiotherapy (RT) is a clinically well-established non-invasive cancer therapy. The protein profile of tumors following bacterial therapy was compared to that of tumors following RT (Jiang *et al.*, 2010). Two groups of CT26 tumor-bearing mice were treated with *Salmonella* (ΔppGpp-Lux, 4×10^7 CFU) or external beam irradiation (twice, with a 4 day interval, for a total 14 Gy) (Fig. 6A). We observed regression of tumor tissue by RT although not as much as that by bacterial therapy. Seven days after treatment, tumor tissues were isolated and protein profiles were determined using specific antibodies (Figs. 6B and 6C). RT resulted in a slight increase in VIME, which was slightly decreased by bacterial therapy. DBNL and TPM3 were significantly decreased by bacterial therapy but not by RT. However, the levels of the three serum proteins TF, HEMO, and HPT were increased in response to both types of therapy. These results suggest that, despite their inducing tumor regression by different mechanisms, RT and bacterial therapy both increase the influx of liver-derived serum proteins to the tumor.

Discussion

Over the past century, many genera of bacteria have been shown to preferentially accumulate in tumors, including *Salmonella*, *Escherichia*, *Clostridium*, *Bifidobacterium*. *Caulobacter*, *Listeria*, *Proteus*, and *Streptococcus* (reviewed in Forbes, 2010). However, not all bacteria are oncolytic: *Salmonella* Typhimurium but not *E. coli* has been shown to be oncolytic, especially against implanted CT26 tumors, in our hands (Jiang *et al.*, 2010; Nguyen *et al.*, 2010). Thus, in this study we have examined the changes in protein expression in CT26 tumors following *Salmonella* treatment to understand the mechanism of tumor regression by bacterial therapy. It was observed that VIME, DBNL, and TPM3, which were reduced following bacterial therapy, participate in cell shape maintenance, in cytoplasm integrity and in the stabilization of cytoskeletal interactions. VIME, a member of the intermediate filament family of proteins, plays an important role in anchoring intracellular organelles in the cytosol (Katsumoto *et al.*, 1990; Fuchs and Weber, 1994). The DBNL/HIP-55 protein possesses putative actin-binding and SH3 domains in its N and C termini (Ensenat *et al.*, 1999). TPM3 binds to actin in the cytoskeleton of non-muscle cells and muscle cells (Clayton *et al.*, 1988). The decrease in the level of these cytoskeletal and morphology-associated proteins in response to bacterial therapy suggests abrupt disruption of tumor tissues and cells by intra-tumoral bacterial proliferation. Further study is needed to understand the down-regulation of these genes following bacterial therapy.

It was intriguing to note that bacterial therapy using *Salmonella* highly induced liver-derived TF, HEMO, and HPT expression, and subsequent transport into tumor tissue, independently of tumor type (Figs. 5A and 5B). It should be noted that expression of these proteins was induced in the liver but they accumulated in the tumor tissue. Thus, the meaning of induction of these proteins is different from their roles as acute-phase proteins, induced following inflammatory stresses. And, this phenomenon was not strain-specific (Fig. 5C). TF is an iron delivery plasma protein (Macedo and de Sousa, 2008). Although iron bound to TF represents less than 0.1% (4 mg) of total body iron, it is the most important iron pool, with a turnover rate of 25 mg/day (Fleming and Bacon, 2005). HEMO is a high-affinity scavenging plasma protein that binds heme released from aged hemoglobin. Thus, HEMO protects the organism from oxidative damage by free heme (Tolosano and Altruda, 2002). HPT, a marker of hemolysis, binds to free hemoglobin released from disrupted red blood cells (Dobryszycka, 1997; Nielsen *et al.*, 2010). It was evident that bacterial therapy resulted in an environment in which free iron and heme might be abundant. In the hypoxic region of tumor tissue in which blood vessels are often disrupted, the frequent infiltration and lysis of red blood cells might be the source of free heme and iron (Leschner *et al.*, 2009). Such an iron-rich environment would favor bacterial growth. To cope with iron-limiting environments, *S. typhimurium* and *E. coli* have evolved to produce and secrete iron-binding siderophores and heme transporters (Wandersman and Delepelaire, 2004). Meanwhile, increased iron and heme following bacterial therapy would create a condition of oxidative toxicity that might result in tissue disruption. Consequently, tumor tissues would mobilize TF, HEMO, and HPT from circulation to reduce free iron and heme. Interestingly, these proteins were highly induced in the liver of mice having undergone bacterial therapy (Dobryszycka, 1997; Tolosano and Altruda, 2002; Macedo and de Sousa, 2008). Various cytokines expressed by activated macrophages following bacterial therapy might induce the expression of these proteins in liver tissue (Leschner *et al.*, 2009).

Although both RT and bacterial therapies achieve tumor regression, the mechanisms underlying regression seem vastly different based on the observation that VIME, DBNL, and TPM3 were decreased by bacterial therapy but not by RT (Fig. 6). Bacteria localize to hypoxic and necrotic regions within tumors while radiation causes apoptosis of proliferating cells (Min *et al.*, 2008a; Thoms and Bristow, 2010). Despite different antitumor mechanisms, it was interesting to observe a similar increase in the serum proteins TF, HEMO and HPT by the two types of therapy. These data suggest that a common mechanism such as hemolysis in the tumor tissue may govern the induction of these proteins in liver. Additional studies are required to fully elucidate the mechanisms underlying tumor regression by bacterial therapy.

Acknowledgements

We thank Dr. R. M. Hoffman for providing the *S. typhimurium* strain A1R. This study was supported by a Korea

Science and Engineering Foundation grant funded by the Regional Technology Innovation Program (RTI05-01-01) of the Ministry of Knowledge Economy, Republic of Korea. H. E. Choy was supported by National Research Foundation of Korea (NRF) (2011-0029942) and C. H. Jung by Special Research Program, CNU (2009). J. J. Min was supported by NRF (2011-0029941) and the Pioneer Research Center Program "Bacteriobot" through NRF funded by MOST (2010-0002241).

References

Agrawal, N., Bettegowda, C., Cheong, I., Geschwind, J.F., Drake, C.G., Hipkiss, E.L., Tatsumi, M., Dang, L.H., Diaz, L.A.Jr., Pomper, M., and *et al.* 2004. Bacteriolytic therapy can generate a potent immune response against experimental tumors. *Proc. Natl. Acad. Sci. USA* **101**, 15172–15177.

Bensadoun, A. and Weinstein, D. 1976. Assay of proteins in the presence of interfering materials. *Anal. Biochem.* **70**, 241–250.

Clayton, L., Reinach, F.C., Chumbley, G.M., and MacLeod, A.R. 1988. Organization of the hTM_{nm} gene. Implications for the evolution of muscle and non-muscle tropomyosins. *J. Mol. Biol.* **201**, 507–515.

Dobryszycka, W. 1997. Biological functions of haptoglobin–new pieces to an old puzzle. *Eur. J. Clin. Chem. Clin. Biochem.* **35**, 647–654.

Ensenat, D., Yao, Z., Wang, X.S., Kori, R., Zhou, G., Lee, S.C., and Tan, T.H. 1999. A novel src homology 3 domain-containing adaptor protein, HIP-55, that interacts with hematopoietic progenitor kinase 1. *J. Biol. Chem.* **274**, 33945–33950.

Fleming, R.E. and Bacon, B.R. 2005. Orchestration of iron homeostasis. *N. Engl. J. Med.* **352**, 1741–1744.

Forbes, N.S. 2010. Engineering the perfect (bacterial) cancer therapy. *Nat. Rev. Cancer* **10**, 785–794.

Fuchs, E. and Weber, K. 1994. Intermediate filaments: structure, dynamics, function, and disease. *Annu. Rev. Biochem.* **63**, 345–382.

Granvogl, B., Ploscher, M., and Eichacker, L.A. 2007. Sample preparation by in-gel digestion for mass spectrometry-based proteomics. *Anal. Bioanal. Chem.* **389**, 991–1002.

Han, J., Shui, J.W., Zhang, X., Zheng, B., Han, S., and Tan, T.H. 2005. HIP-55 is important for T-cell proliferation, cytokine production, and immune responses. *Mol. Cell. Biol.* **25**, 6869–6878.

Jain, R.K. and Forbes, N.S. 2001. Can engineered bacteria help control cancer? *Proc. Natl. Acad. Sci. USA* **98**, 14748–14750.

Jiang, S.N., Phan, T.X., Nam, T.K., Nguyen, V.H., Kim, H.S., Bom, H.S., Choy, H.E., Hong, Y., and Min, J.J. 2010. Inhibition of tumor growth and metastasis by a combination of *Escherichia coli*-mediated cytolytic therapy and radiotherapy. *Mol. Ther.* **18**, 635–642.

Katsumoto, T., Mitsushima, A., and Kurimura, T. 1990. The role of the vimentin intermediate filaments in rat 3Y1 cells elucidated by immunoelectron microscopy and computer-graphic reconstruction. *Biol. Cell* **68**, 139–146.

Kimura, N.T., Taniguchi, S., Aoki, K., and Baba, T. 1980. Selective localization and growth of *Bifidobacterium bifidum* in mouse tumors following intravenous administration. *Cancer Res.* **40**, 2061–2068.

Leschner, S., Westphal, K., Dietrich, N., Viegas, N., Jablonska, J., Lyszkiewicz, M., Lienenklaus, S., Falk, W., Gekara, N., Loessner, H., and *et al.* 2009. Tumor invasion of *Salmonella enterica* serovar Typhimurium is accompanied by strong hemorrhage promoted by TNF-alpha. *PLoS ONE* **4**, e6692.

Low, K.B., Ittensohn, M., Luo, X., Zheng, L.M., King, I., Pawelek, J.M., and Bermudes, D. 2004. Construction of VNP20009: a novel, genetically stable antibiotic-sensitive strain of tumor-targeting Salmonella for parenteral administration in humans. *Methods Mol. Med.* **90**, 47–60.

Macedo, M.F. and de Sousa, M. 2008. Transferrin and the transferrin receptor: of magic bullets and other concerns. *Inflamm. Allergy Drug Targets* **7**, 41–52.

Min, J.J., Kim, H.J., Park, J.H., Moon, S., Jeong, J.H., Hong, Y.J., Cho, K.O., Nam, J.H., Kim, N., Park, Y.K., and *et al.* 2008a. Noninvasive real-time imaging of tumors and metastases using tumor-targeting light-emitting *Escherichia coli*. *Mol. Imaging Biol.* **10**, 54–61.

Min, J.J., Nguyen, V.H., and Gambhir, S.S. 2010. Molecular imaging of biological gene delivery vehicles for targeted cancer therapy: Beyond viral vectors. *Nucleic Med. Mol. Imaging* **44**, 15–24.

Min, J.J., Nguyen, V.H., Kim, H.J., Hong, Y., and Choy, H.E. 2008b. Quantitative bioluminescence imaging of tumor-targeting bacteria in living animals. *Nat. Protoc.* **3**, 629–636.

Na, H.S., Kim, H.J., Lee, H.C., Hong, Y., Rhee, J.H., and Choy, H.E. 2006. Immune response induced by *Salmonella typhimurium* defective in ppGpp synthesis. *Vaccine* **24**, 2027–2034.

Nguyen, V.H., Kim, H.S., Ha, J.M., Hong, Y., Choy, H.E., and Min, J.J. 2010. Genetically engineered *Salmonella typhimurium* as an imageable therapeutic probe for cancer. *Cancer Res.* **70**, 18–23.

Nielsen, M.J., Moller, H.J., and Moestrup, S.K. 2010. Hemoglobin and heme scavenger receptors. *Antioxid. Redox. Signal* **12**, 261–273.

Pawelek, J.M., Low, K.B., and Bermudes, D. 1997. Tumor-targeted Salmonella as a novel anticancer vector. *Cancer Res.* **57**, 4537–4544.

Ryan, R.M., Green, J., and Lewis, C.E. 2006. Use of bacteria in anticancer therapies. *Bioessays* **28**, 84–94.

Ryan, R.M., Green, J., Williams, P.J., Tazzyman, S., Hunt, S., Harmey, J.H., Kehoe, S.C., and Lewis, C.E. 2009. Bacterial delivery of a novel cytolysin to hypoxic areas of solid tumors. *Gene Ther.* **16**, 329–339.

Song, M., Kim, H.J., Kim, E.Y., Shin, M., Lee, H.C., Hong, Y., Rhee, J.H., Yoon, H., Ryu, S., Lim, S., and *et al.* 2004. ppGpp-dependent stationary phase induction of genes on Salmonella pathogenicity island 1. *J. Biol. Chem.* **279**, 34183–34190.

Taniguchi, S., Fujimori, M., Sasaki, T., Tsutsui, H., Shimatani, Y., Seki, K., and Amano, J. 2010. Targeting solid tumors with non-pathogenic obligate anaerobic bacteria. *Cancer Sci.* **101**, 1925–1932.

Thamm, D.H., Kurzman, I.D., King, I., Li, Z., Sznol, M., Dubielzig, R.R., Vail, D.M., and MacEwen, E.G. 2005. Systemic administration of an attenuated, tumor-targeting *Salmonella typhimurium* to dogs with spontaneous neoplasia: phase I evaluation. *Clin. Cancer Res.* **11**, 4827–4834.

Thoms, J. and Bristow, R.G. 2010. DNA repair targeting and radiotherapy: a focus on the therapeutic ratio. *Semin. Radiat. Oncol.* **20**, 217–222.

Tolosano, E. and Altruda, F. 2002. Hemopexin: structure, function, and regulation. *DNA Cell Biol.* **21**, 297–306.

Toso, J.F., Gill, V.J., Hwu, P., Marincola, F.M., Restifo, N.P., Schwartzentruber, D.J., Sherry, R.M., Topalian, S.L., Yang, J.C., Stock, F., and *et al.* 2002. Phase I study of the intravenous administration of attenuated *Salmonella typhimurium* to patients with metastatic melanoma. *J. Clin. Oncol.* **20**, 142–152.

Wandersman, C. and Delepelaire, P. 2004. Bacterial iron sources: from siderophores to hemophores. *Annu. Rev. Microbiol.* **58**, 611–647.

Weibel, S., Stritzker, J., Eck, M., Goebel, W., and Szalay, A.A. 2008. Colonization of experimental murine breast tumours by *Escherichia coli* K-12 significantly alters the tumour micro-

environment. *Cell Microbiol.* **10**, 1235–1248.

Yu, Y.A., Shabahang, S., Timiryasova, T.M., Zhang, Q., Beltz, R., Gentschev, I., Goebel, W., and Szalay, A.A. 2004. Visualization of tumors and metastases in live animals with bacteria and vaccinia virus encoding light-emitting proteins. *Nat. Biotechnol.* **22**, 313–320.

Zhao, M., Yang, M., Li, X.M., Jiang, P., Baranov, E., Li, S., Xu, M., Penman, S., and Hoffman, R.M. 2005. Tumor-targeting bacterial therapy with amino acid auxotrophs of GFP-expressing *Salmonella typhimurium*. *Proc. Natl. Acad. Sci. USA* **102**, 755–760.

Zhao, M., Yang, M., Ma, H., Li, X., Tan, X., Li, S., Yang, Z., and Hoffman, R.M. 2006. Targeted therapy with a *Salmonella typhimurium* leucine-arginine auxotroph cures orthotopic human breast tumors in nude mice. *Cancer Res.* **66**, 7647–7652.